International Journal of Thermal Sciences 99 (2016) 41–51

Contents lists available at ScienceDirect

International Journal of Thermal Sciences

journal homepage: www.elsevier.com/locate/ijts

Numerical study of laminar natural convection inside square enclosure with single horizontal fin

Ahmed Elatar [a, b, *], Mohamed A. Teamah [a], Mohamed A. Hassab [a]

[a] Department of Mechanical Engineering, Faculty of Engineering, Alexandria University, Egypt
[b] Department of Mechanical and Materials Engineering, The University of Western Ontario, Canada

ARTICLE INFO

Article history:
Received 1 February 2015
Received in revised form
2 August 2015
Accepted 5 August 2015
Available online 29 August 2015

Keywords:
Natural convection
Square enclosure
Horizontal fin

ABSTRACT

A numerical study for laminar natural convection inside a square enclosure with a single horizontal fin attached to its hot wall has been carried out. The enclosure horizontal surfaces are adiabatic, the left wall is hot while the right one is cold. The Prandtl number for the flow inside the enclosure is 0.71. A parametric study has been carried out to investigate the effect of Rayleigh number, fin length, conductivity ratio, thickness and position on heat transfer. The fin thickness showed negligible effect on the average Nusselt number for all values of fin conductivity ratios. The fin efficiency and temperature distribution were examined. The fin effectiveness was also studied and it was found that the fin effectiveness enhanced in general with the increase of fin length. Also, the maximum fin effectiveness was found at the lowest Rayleigh number for a given fin conductivity ratio. A correlation has been proposed for the relation between Nusselt number and the parameters of study.

1. Introduction

Natural convection inside a cavity with different boundary conditions has been studied extensively with and without fin/partition in the last few decades due to its importance and the several applications that can be simplified into such a model. This type of research can be applied in different applications such as double glass windows, cooling of nuclear reactors, solar collectors and electronic equipment to name a few.

Natural convection inside cavities has been examined extensively for different boundary conditions, aspect ratios and Rayleigh numbers [1–8]. It was also examined inside cavities with the employment of heating elements [9–12]. Adding a fin inside the enclosure has a significant effect on both flow field and heat transfer and many studies have investigated heat transfer behavior under such condition. Frederick [13] studied numerically natural convection in a differentially heated inclined square enclosure with a fin attached to the cold vertical wall. Bilgen [14] studied numerically natural convection heat transfer inside a differentially heated cavity (left heated wall and cooled right wall) with a horizontal fin attached to the hot wall. It was found that the fin position has a major role in heat transfer inside the cavity. It was also found that the heat transfer rate was minimum with the fin attached to the center or near the center of the wall. Shi and Khodadadi [15] studied numerically steady laminar natural convection within a differentially heated square cavity with a thin fin attached to the hot wall. They found that for high Rayleigh numbers, heat transfer was enhanced regardless of the position or the length of the fin. Frederick and Valencia [16] studied numerically heat transfer in a square cavity with conducting horizontal surfaces. A conducting horizontal partition was attached to the center of the hot wall. It was found that increasing thermal conductivity ratio enhanced heat transfer.

Nag et al. [17] studied numerically natural convection in a differentially heated square enclosure with a horizontal fin attached to the hot wall. The study was done for two cases: a highly conductive fin and an adiabatic fin. For the case of highly conductive fin, it was found that the Nusselt number on the cold wall increased compared to the case with no fin. For the case with the adiabatic fin, heat transfer was reduced compared to the case without a fin. Tasnim and Collins [18] investigated numerically natural convection of air inside a square enclosure with left heated wall, right cold wall and two horizontal adiabatic walls. A highly conductive fin was attached to the hot wall. The study

* Corresponding author. Department of Mechanical and Materials Engineering, The University of Western Ontario, Canada. Tel.: +20 519 777 3144.
E-mail address: aelatar@uwo.ca (A. Elatar).

http://dx.doi.org/10.1016/j.ijthermalsci.2015.08.003
1290-0729/

Nomenclatures

b	fin thickness
B	dimensionless fin thickness, b/W
g	gravitational acceleration,
Gr	Grashof number, $W^3\ g\ \beta\ (T_h - T_c)/\nu^2$
h^*	heat transfer coefficient
h	fin position
H	dimensionless fin position, h/W
k	thermal conductivity
l	fin length
L	dimensionless fin length, (l/W)
n	distance normal to S coordinate
N	dimensionless distance normal to S coordinates (n/W)
Nu_{av}	average Nusselt number
Nu_L	local Nusselt number
p	pressure
P	dimensionless pressure, $(p\ W^2/\rho\ \alpha^2)$
Pr	Prandtl number, (ν/α).
Ra	Rayleigh number, (Gr * Pr)
R_k	conductivity ratio, (k_f/k_a)
S	dimensionless special coordinate along enclosure surface
T	temperature
u, v	velocity components in X and Y direction respectively,
U, V	dimensionless velocity in X and Y direction respectively, $(U = u\ W/\alpha)$ and $(V = v\ W/\alpha)$
W	enclosure width and height
x	horizontal coordinate
X	dimensionless horizontal coordinate (x/W)
y	vertical coordinate
Y	dimensionless vertical coordinate (y/W)

Greek symbols

α	thermal diffusivity,
ρ	local density,
β	coefficient of thermal expansion
μ	dynamic viscosity
ν	kinematic viscosity, (μ/ρ)
θ	dimensionless temperature $(T - T_c)/(T_h - T_c)$
ε	fin effectiveness, (Q_{fin}/Q_{nofin})
η	fin efficiency, $(Q_{real}/Q_{isothermal})$

Subscripts

av	average
a	air
f	fin

showed that the presence of a fin always increases heat transfer. They found that the effect of fin position on the heat transfer rate was strongly affected by Rayleigh number and the fin length. Ben-Nakhi and Chamkha [19] studied numerically steady laminar natural convection inside an enclosure with a highly conductive inclined fin attached to its hot wall and adiabatic horizontal walls. It was found that the effect of fin inclination angle was dependent on the fin length. Ben-Nakhi and Chamkha [20] also studied numerically conjugate natural convection inside an enclosure with three thick cold walls and a hot thin vertical left wall. They found that increasing the thermal conductivity and decreasing the fin length enhanced the average Nusselt number on the hot wall, while increasing the fin length enhanced the average Nusselt number on cold surfaces. Shi and Khodadadi [21] studied heat transfer inside a led-driven cavity with a fin attached perpendicular to any of the three stationary surfaces. They concluded that the fin slowed the flow near the anchoring wall and reduces the temperature gradient, thus the heat transfer capacity was degraded. Oztop and Bilgen [22] studied numerically heat transfer in a differentially heated square cavity with adiabatic horizontal walls and internal heat generation. An isothermal partition was vertically attached on the bottom wall. The study has shown that increasing both thickness and length of the cold partition reduce heat transfer rate. Bilgen [23] studied a differentially heated enclosure with partial partitions attached vertically to the top and bottom adiabatic walls. It was concluded that up to $Ra = 10^8$, laminar flow regime was found while turbulent flow regime starts to be formed for higher values of Rayleigh number.

Three-dimensional study of natural convection for air inside a cubic enclosure with a thick fin attached to the hot left wall was conducted by Frederick and Moraga [24]. The right wall was kept cold and the two horizontal walls were adiabatic. The study showed that by increasing thermal conductivity ratio between the fin material and the air inside the enclosure, the cell was displaced away from the hot wall and the blockage effect was reduced. They also found that for a high conductivity ratio, 20% enhancement of heat transfer was obtained compared to the cube without a fin.

As seen from the literature, natural convection inside enclosure has been studied for different boundary conditions with or without fins attached. However, no significant work has been conducted to investigate the effect of the fin thermal conductivity and fin thickness inside a differentially heated square enclosure. In addition, the fin efficiency and effectiveness are two important parameters under such circumstances; however, there was not a detailed investigation of these parameters under different fin design conditions. The aim of this study is to investigate steady two-dimensional laminar natural convection inside an enclosure with a horizontal fin attached to the hot wall. A parametric study will be conducted to investigate the effect of fin thickness, fin thermal conductivity, length and position on heat transfer inside the enclosure at different values of Rayleigh number. In addition, the fin performance in terms of efficiency and effectiveness will be investigated.

2. Mathematical model

The physical model and coordinate system under consideration are schematically shown in Fig. 1 which represents a two-dimensional square enclosure. The left wall is maintained at a high temperature T_h, the right wall is kept at a low temperature T_c $(T_h > T_c)$ and the two horizontal surfaces are insulated. The side length of the enclosure is (W). A horizontal fin is attached to the hot left wall with a length (l) at a position (h) from the bottom surface and thickness (b). The fin is assumed to exchange heat by convection with the surrounding fluid (radiation, if it exists, is lumped with convection). The fluid inside the space is assumed to be Newtonian and incompressible (constant property fluid) except for the density in the buoyancy force components existing in the momentum equations. The Boussinesq approximation is applied, which relates the density to the local temperature of the fluid. Consequently, the momentum equations will be coupled with the energy equation.

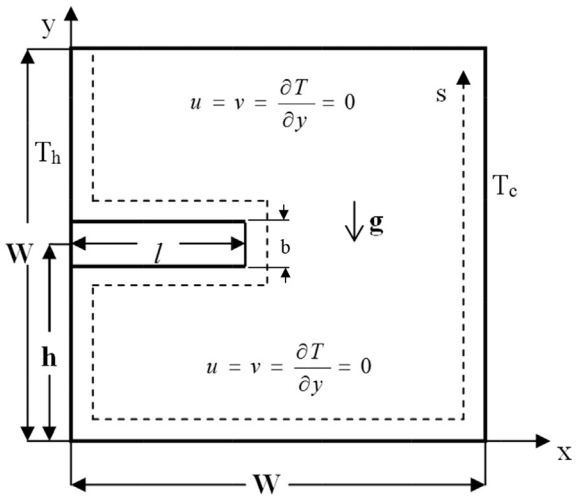

Fig. 1. A schematic diagram for the problem with boundary conditions.

The governing equations for the problem under consideration are based on the balance laws of mass, linear momentum and energy in two dimensions and steady state. Following the previous assumptions, these equations can be written in dimensional form as;

$$\frac{\partial \boldsymbol{u}}{\partial \boldsymbol{x}} + \frac{\partial \boldsymbol{v}}{\partial \boldsymbol{y}} = 0 \tag{1}$$

$$u\frac{\partial u}{\partial x} + v\frac{\partial u}{\partial y} = -\frac{1}{\rho}\frac{\partial p}{\partial x} + \nu\left(\frac{\partial^2 u}{\partial x^2} + \frac{\partial^2 u}{\partial y^2}\right) \tag{2}$$

$$u\frac{\partial v}{\partial x} + v\frac{\partial v}{\partial y} = g\frac{\rho}{\rho_o} - \frac{1}{\rho_o}\frac{\partial p}{\partial y} + \nu\left(\frac{\partial^2 v}{\partial x^2} + \frac{\partial^2 v}{\partial y^2}\right) \tag{3}$$

$$u\frac{\partial T}{\partial x} + v\frac{\partial T}{\partial y} = \alpha\left(\frac{\partial^2 T}{\partial x^2} + \frac{\partial^2 T}{\partial y^2}\right) \tag{4}$$

The boundary conditions for the calculation domain in the dimensional form are;

at x = 0.0; u = v = 0.0, T = T_h, at x = W; u = v = 0.0, T = T_c
at y = 0.0; u = v = 0.0, $\frac{\partial T}{\partial y} = 0.0$, at y = W; u = v = 0.0, $\frac{\partial T}{\partial y} = 0.0$

While for the fin surface;

at $0 \le x \le l$, $y = h + b/2$ and $y = h - b/2$; u = v = 0.0, $k_f\left(\frac{\partial T}{\partial y}\right)_f = k_a\left(\frac{\partial T}{\partial y}\right)_a$
at $h - b/2 \le y \le h + b/2$, x = l; u = v = 0.0, $k_f\left(\frac{\partial T}{\partial x}\right)_f = k_a\left(\frac{\partial T}{\partial x}\right)_a$

and introducing the following dimensionless groups for the governing equations,

$$X = \frac{x}{W}, \quad Y = \frac{y}{W}, \quad H = \frac{h}{W}, \quad L = \frac{l}{W}, \quad B = \frac{b}{W}$$
$$U = \frac{uW}{\alpha}, \quad V = \frac{\nu W}{\alpha}, \quad P = \frac{pW^2}{\rho\alpha^2}, \quad \theta = \frac{T - T_c}{T_h - T_c} \tag{5}$$

A set of governing equations is obtained as:

$$\frac{\partial U}{\partial X} + \frac{\partial V}{\partial Y} = 0 \tag{6}$$

$$U\frac{\partial U}{\partial X} + V\frac{\partial U}{\partial Y} = \Pr\left(\frac{\partial^2 U}{\partial X^2} + \frac{\partial^2 U}{\partial Y^2}\right) - \frac{\partial P}{\partial X} \tag{7}$$

$$U\frac{\partial V}{\partial X} + V\frac{\partial V}{\partial Y} = \Pr\left(\frac{\partial^2 V}{\partial X^2} + \frac{\partial^2 V}{\partial Y^2}\right) - \frac{\partial P}{\partial Y} + Ra^*\Pr^*\theta \tag{8}$$

$$U\frac{\partial \theta}{\partial X} + V\frac{\partial \theta}{\partial Y} = \left(\frac{\partial^2 \theta}{\partial X^2} + \frac{\partial^2 \theta}{\partial Y^2}\right) \tag{9}$$

For the fin, the energy equation is reduced to

$$\frac{\partial^2 \theta}{\partial X^2} + \frac{\partial^2 \theta}{\partial Y^2} = 0 \tag{10}$$

where *Pr*, *Gr*, *Ra*, ν and α are respectively Prandtl number, Grashof number, Rayleigh number, kinematic viscosity and thermal diffusivity and they are defined as:

$$\alpha = \frac{k}{\rho C_P}, \quad \nu = \frac{\mu}{\rho}, \quad Pr = \frac{\nu}{\alpha}$$
$$Gr = \frac{W^3 g\beta(T_h - T_c)}{\nu^2}, \quad Ra = Gr^*Pr$$

The boundary conditions for the calculation domain in dimensionless form are:

at $X = 0.0$; $U = V = 0.0$, $\theta = 1.0$, at $X = 1.0$; $U = V = 0.0$, $\theta = 0.0$
at $Y = 0.0$; $U = V = 0.0$, $\frac{\partial \theta}{\partial Y} = 0.0$, at $Y = 1.0$; $U = V = 0.0$, $\frac{\partial \theta}{\partial Y} = 0.0$

While for the fin surface;

at $0 \le X \le L$, $Y = H + B/2$ and $Y = H - B/2$; $U = V = 0.0$, $R_k\left(\frac{\partial \theta}{\partial Y}\right)_f = \left(\frac{\partial \theta}{\partial Y}\right)_a$
at $H - B/2 \le Y \le H + B/2$, $X = L$; $U = V = 0.0$, $R_k\left(\frac{\partial \theta}{\partial X}\right)_f = \left(\frac{\partial \theta}{\partial X}\right)_a$

2.1. Nusselt number

First, the heat transfer by conduction was equated to the heat transfer by convection:

$$h^*\Delta T = -k\frac{\partial T}{\partial n} \tag{11}$$

where n is the normal distance to the coordinate s. By introducing the dimensionless variables, defined in eq. (5) into eq. (11), Nusselt number is defined as:

$$Nu_L = -\left.\frac{\partial \theta}{\partial N}\right|_{surface} \tag{12}$$

The average Nusselt number on the cold wall is obtained by integrating the above local Nusselt number over the cold wall

$$Nu_{av} = -\int_{2+2L}^{3+2L} \left.\frac{\partial \theta}{\partial N}\right|_{surface} dS \tag{13}$$

3. Solution procedure

The governing equations were solved using the finite volume technique developed by Patanker [25]. This technique was based on the discretization of the governing equations using the central difference in space. The discretization equations were solved by the Gauss-Seidel method. The iteration method used in this program is a line-by-line procedure, which is a combination of the direct method and the resulting Tri Diagonal Matrix Algorithm (TDMA). The accuracy was checked and it was found that 1500 iterations were enough to reach stable solution. Fig. 2(a) shows the convergence and stability of the solution. The number of nodes used was checked. Fig. 2(b) presents the dependence of average Nusselt number on the number of nodes. It can be shown that two numbers of nodes of 7500 and 9375 give nearly identical results. Considering both the accuracy and the computational time, 7500 nodes were used; where 75 nodes are used in the X direction and 100 nodes in the Y direction. The node is located half way between two adjacent control volume faces and a uniform grid was taken in both directions.

4. Program validation and comparison with previous research

In order to check the accuracy of the numerical results obtained in this problem, a comparison is made between results of the average Nusselt number of the present work with other researches for enclosure without a fin as shown in Table 1. The maximum deviation was 1.45% for the case of $Ra = 10^6$.

Furthermore, the average Nusselt number along the right cold wall was compared with the results presented by Nag. et al. [26] for natural convection inside a cavity with a thick fin attached to the left hot wall. The Nusselt number values as seen in Table 2 show good agreement between both studies with maximum deviation of less than 2%.

In addition, a comparison of the streamlines and the isothermal lines is made between the present work and Tasnim and Collins [23] at ($Ra = 10^5$, $R_k = 10{,}000$, $B = 0.01$, $L = 0.5$ and $H = 0.75$) as shown in Fig. 3. The shapes of streamlines contours are almost identical. For the isotherms, one can see the strong agreement of present work with that by Tasnim and Collins [23] as seen in the figure.

5. Results and discussion

In the present study, different parameters were examined to study their effect on the heat transfer process inside the enclosure as follows: Rayleigh number ranged between 10^3 and 10^6, fin length (L) and position (H) were in the range between 0.125 and 0.875, fin thickness (B) varied between 0.02 and 0.1 and the fin conductivity ratio values considered were 10,100 and 1000. Prandtl number of 0.71 was considered for the flow inside the enclosure.

Table 1
Comparison of average Nusselt number on the left or right wall without a fin with references [15,17,18,23].

Ra	10^4	10^5	10^6
Nag et al. [17]	2.240	4.510	8.820
Shi and Khodadadi [15]	2.247	4.532	8.893
Ben-Nakhi and Chamkha [18]	2.244	4.524	8.856
Tasnim and Collins [23]	2.244	4.5236	8.8554
Present work	2.234	4.517	8.948

Table 2
Comparison of average Nusselt number on the cold wall for $R_k = 7750$, $L = 0.2$ and $Ra = 10^6$.

B	0.02	0.04	0.1
Nag et al. [26]	8.861	8.888	9.033
Present work	8.672	8.71	8.947

The streamlines and isothermal lines are presented in Figs. 4 and 5 for $Ra = 10^4$ with fin length values of ($L = 0.25$, 0.5 and 0.75) attached at different positions ($H = 0.25$, 0.5 and 0.75); the fin conductivity ratio is $R_k = 1000$ with thickness $B = 0.04$. One can see from Fig. 4 that the fin is blocking the vortex below and above the fin surface for $H = 0.25$ and 0.75 respectively. It is also noticed that as the fin length increases, the vortex is weakened due to the blockage effect for all fin positions. The vortex became stronger as the Rayleigh number increases (figures not shown). At $Ra = 10^6$, the vortex becomes strong enough to overcome the fin blockage effect and occupies the areas below the fin for $H = 0.25$ and above it for $H = 0.75$. Thus, heat transfer enhancement is expected in these areas. One can also notice that longer fin have a greater effect than the shorter one for all the cases studied.

Fig. 5 shows isotherms for $Ra = 10^4$. The isotherms are skewed which implies that heat transfer by convection is presented in addition to heat conduction. The regions of low isotherms concentration are the regions of low heat transfer (e.g. the region above the fin for $H = 0.75$). Isotherms in the upper half along the right wall are dense which indicates high heat transfer at this area. This can be seen strongly for fin length $L = 0.75$ at different fin positions. With the increase of Rayleigh number, the isotherms become more packed and the thermal boundary layer becomes denser along the right cold wall, the left hot wall below the fin and the lower fin surface (figures not shown here). It is also found that increasing the fin length ($L = 0.5$ and 0.75) and height ($H = 0.5$ and 0.75) reduces the isotherms density in the region above the fin, especially for higher Rayleigh numbers which indicates lower heat transfer in this area.

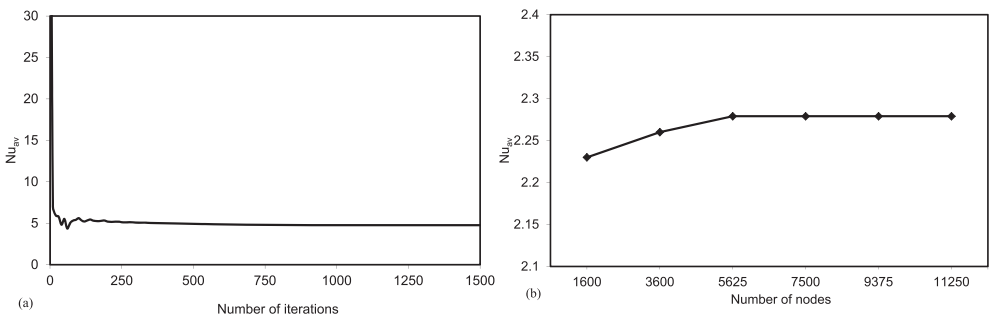

Fig. 2. Effect of number of (a) iterations and (b) nodes on average Nusselt number.

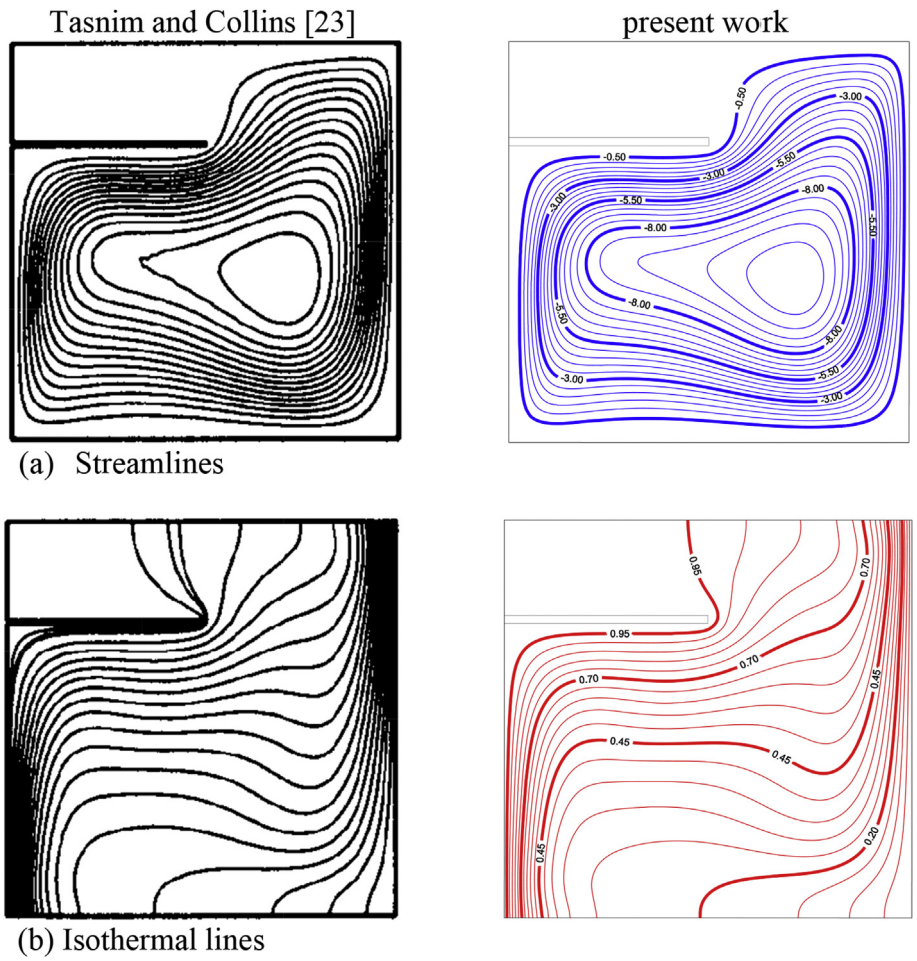

Fig. 3. Comparison of streamlines and isotherms with those given by Tasnim and Collins [23], ($Ra = 10^5$, $R_k = 10{,}000$, $B = 0.01$, $L = 0.5$ and $H = 0.75$).

As the fin plays a significant role in heat transfer inside the enclosure, we found that detailed analyses of the fin should be conducted. Fig. 6 shows the temperature (θ_f) distribution along the fin for different values of R_k at $H = 0.5$ and $Ra = 10^6$. It can be seen that the fin temperature at any location increases with the increase of R_k. This is due to the decrease of the fin conductive resistance with the increase of R_k which leads to the increase of the fin temperature along the entire surface. As the fin length increases, the fin temperature decreases for all values of R_k. It can also be seen that for fin with $R_k = 10$ and 100, the fin temperature decreasing rate is higher compared to the fin with $R_k = 1000$. The dimensionless fin tip temperatures for $R_k = 10$, 100 and 1000 dropped to 0.57, 0.77 and 0.98 respectively.

The fin efficiency is the ratio between heat transferred from the fin in the real case (i.e. fin temperature drops along the length) and heat transferred from the fin for the case of an isothermal fin ($\theta_f = 1$) and defined as follows:

$$\eta_f = \frac{Q_{real}}{Q_{isothermal}} \tag{14}$$

Fig. 7 presents the fin efficiency as a function of the fin length for ($Ra = 10^6$, $H = 0.5$, $B = 0.04$) for different values of fin thermal conductivity ratio. The figure shows that at a given fin length, the fin efficiency decreases with the decrease of R_k as a result of fin temperature decrease, which is expected. It is also noticed that with the increase of the fin length, the fin efficiency also decreases due to the decrease of fin temperature. The rate of fin efficiency decrease with the fin length is higher for low R_k while, it is lower for high R_k. The results in Fig. 7 show the strong connection between the fin temperature and efficiency.

The local Nusselt number distribution along the hot wall (Nu_s), including both fin surfaces and the fin tip, for different values of fin position (H) and Rayleigh number with $L = 0.5$, $R_k = 1000$ and $B = 0.04$ is shown in Fig. 8. Along both fin surfaces, the local Nusselt number value starts to rise along the fin's upper surface until it reaches the fin tip, then starts to fall along the fin's lower surface until it reaches the base of the fin with $Nu_s = 0$. As the fin position rises, the local Nusselt number along the wall below the fin increases while it decreases along the wall above the fin. This can be explained by the given streamlines and isotherms contours shown in Figs. 4 and 5 for the same fin position. The local Nusselt number along both fin surfaces decreases as the fin position (H) rises which also can be explained by the streamlines and isotherms seen in Figs. 4 and 5. Rayleigh number is found to enhance the local Nusselt number along the left hot wall including the fin surfaces as seen in the figure. One can see how the local Nusselt number is linked to the vortex dynamics inside the enclosure and consequently the isothermal lines which are affected by the fin parameters.

To investigate the role of fin thickness on the average Nusselt number, the average Nusselt number (Nu_{av}) as a function of the fin thicknesses is shown in Fig. 9 for $H = 0.5$, $L = 0.5$ and $Ra = 10^5$. It can be seen from the figure that the fin thickness has an overall minor effect on the average Nusselt number.

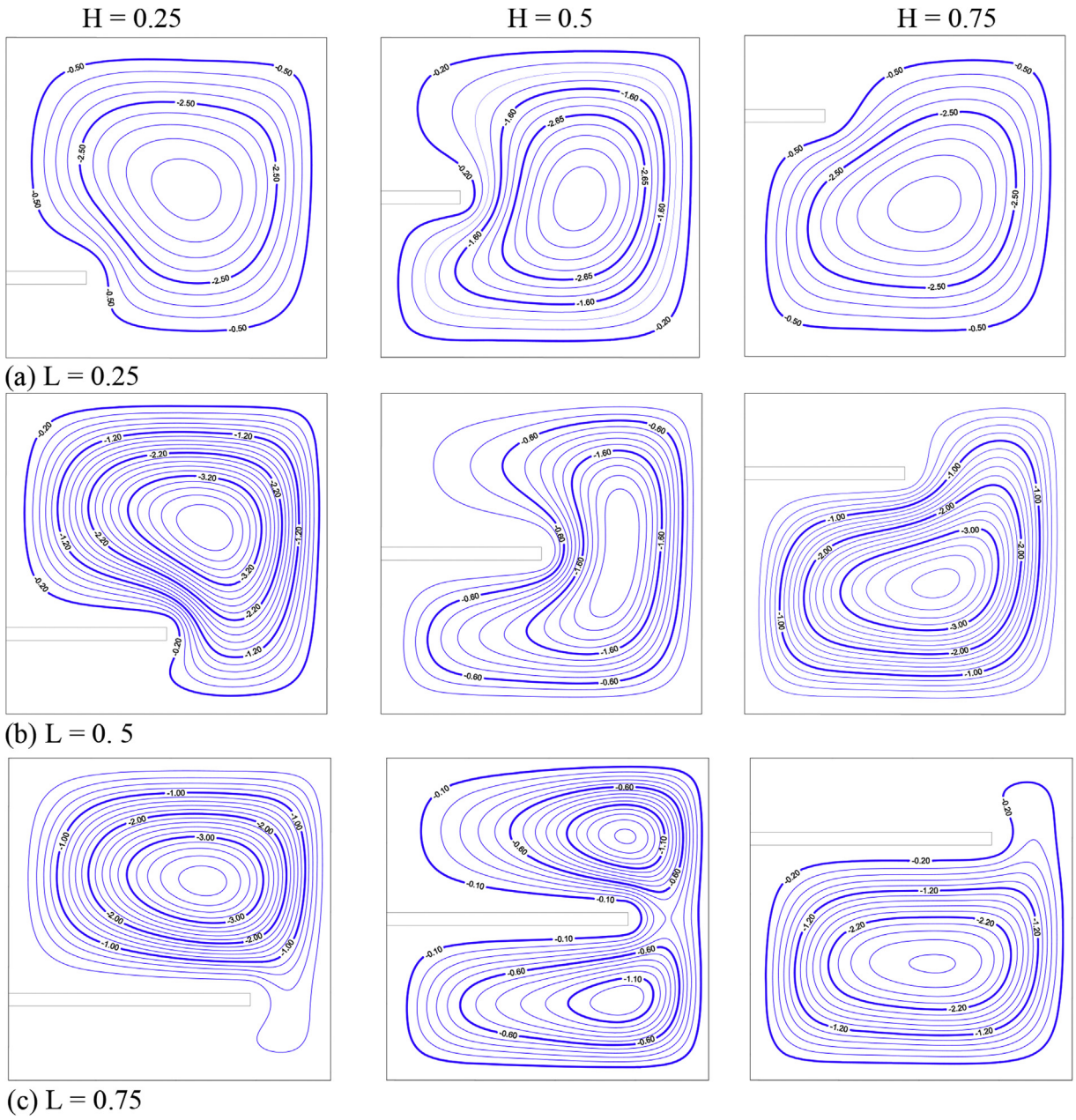

Fig. 4. Streamlines at $Ra = 10^4$.

As the fin thickness increased from 0.02 to 0.1, the average Nusselt number increased by approximately 4% for $R_k = 10$ and 100 as seen in the figure while it is almost constant for $R_k = 1000$. As the fin thickness increases, the contact area between the fin and the left hot wall increases which results in heat transfer enhancement by conduction. However, the temperature gradient across the fin thickness is not significantly improved which yielded a negligible increase in the average Nusselt number. Thus, it can be concluded that the effect of fin thickness is secondary and decreases with the increase of the fin conductivity ratio.

The effect of fin conductivity ratio (R_k) on the average Nusselt number is presented in Fig. 10 for different values of Rayleigh number. One can see that the average Nusselt number increases with the increase of the conductivity ratio from 10 to 1000 by 66%, 63%, 32% and 20% for $Ra = 10^3$, 10^4, 10^5 and 10^6 respectively. This is due to the decrease in the fin conductive resistance with the increase of the fin conductivity ratio. Accordingly, the temperature degradation along the fin decreases which enhances heat transfer. As the conductivity ratio increases beyond 1000, the average Nusselt number shows almost no change as seen in the figure. Thus, the optimum fin conductivity ratio for the current configuration is 1000.

Fin effectiveness (ε_f) is the parameter that quantifies the heat transfer enhancement inside the enclosure with a fin compared to the case with no fin and is defined as follows:

$$\varepsilon_f = \frac{Q_{fin}}{Q_{nofin}} \tag{15}$$

The fin effectiveness is shown in Fig. 11 as a function of fin position (H) for different fin lengths at the lowest conductivity ratio ($R_k = 10$). Fig. 11(a) presents the fin effectiveness at $Ra = 10^3$ and

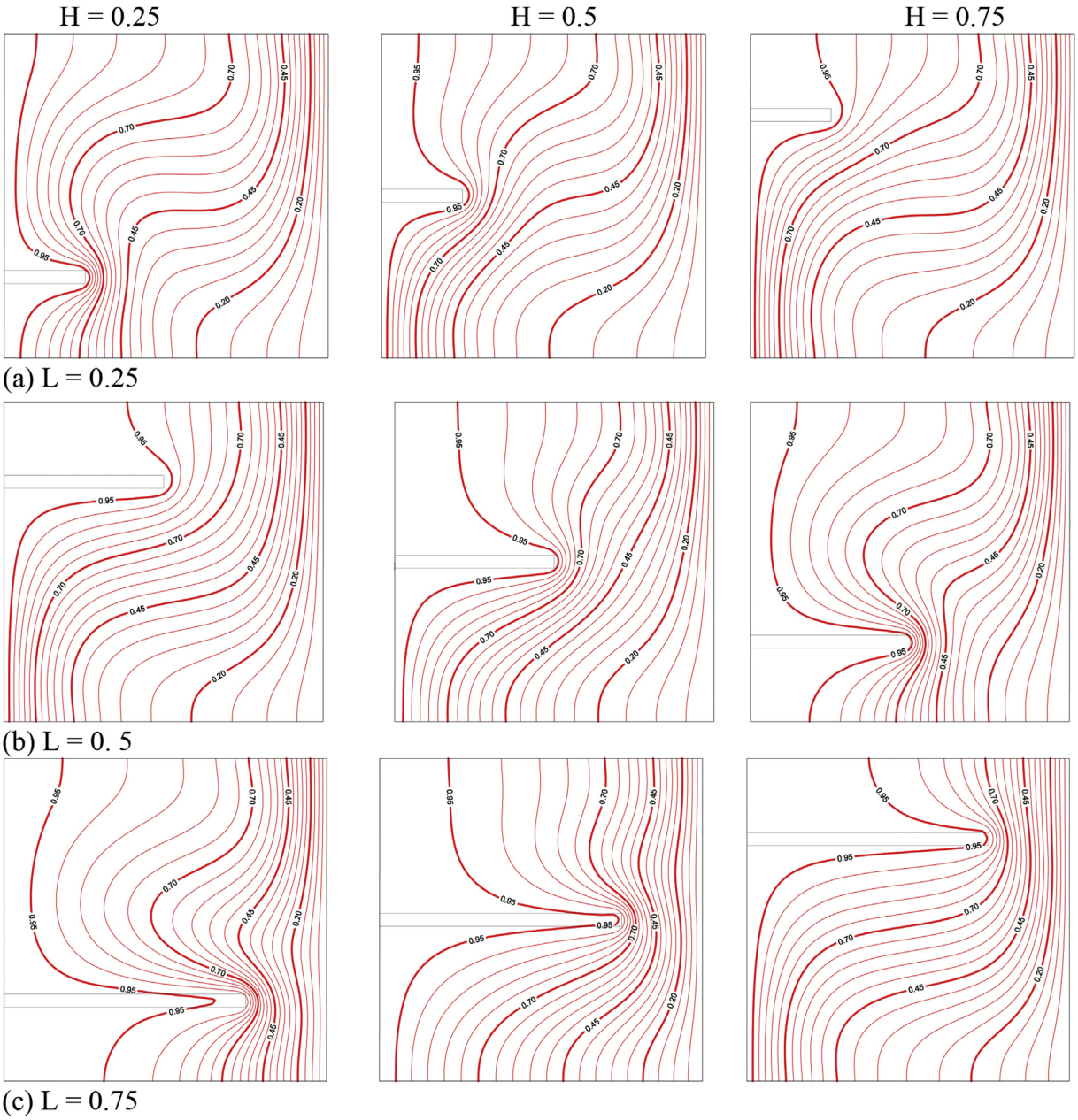

Fig. 5. Isothermal lines at $Ra = 10^4$.

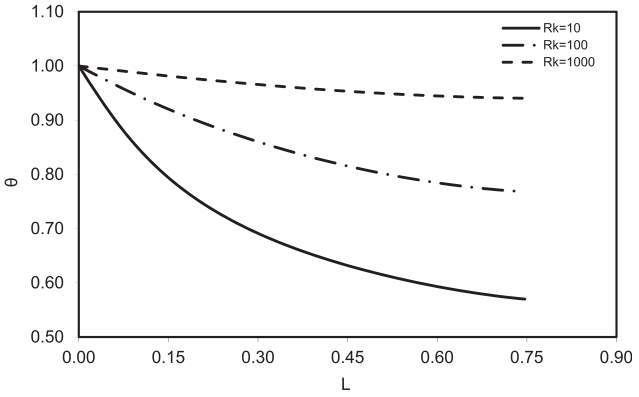

Fig. 6. Fin temperature distribution for ($Ra = 10^6$, $H = 0.5$, $B = 0.04$).

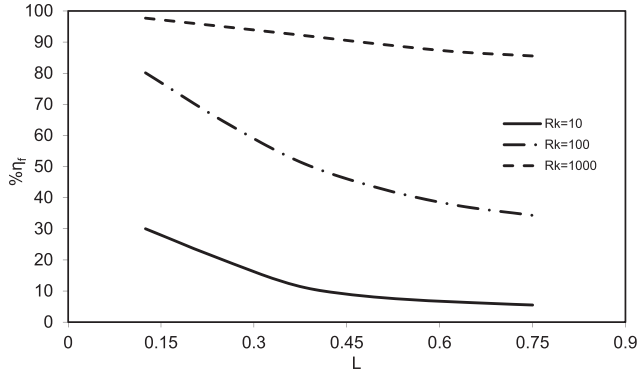

Fig. 7. Fin efficiency as a function of fin length for ($Ra = 10^6$, $H = 0.5$, $B = 0.04$).

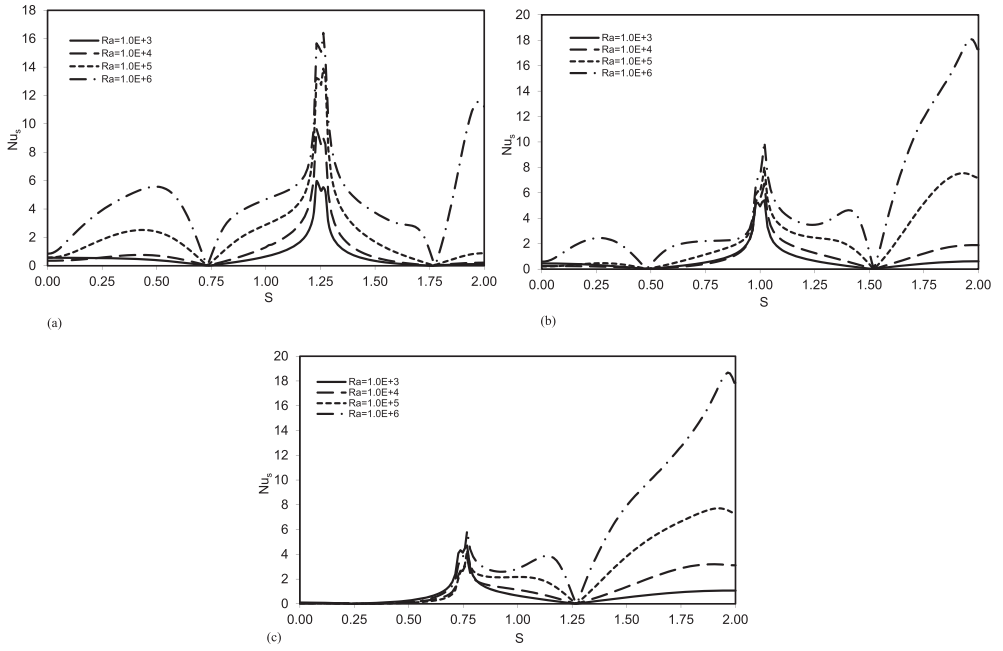

Fig. 8. Variation of local Nusselt number for (a) $H = 0.25$, (b) $H = 0.5$, (c) $H = 0.75$.

shows that the fin position (H) has minor effect on fin effectiveness for all values of fin length (L). In this figure, it is seen that $\varepsilon_f > 1$ for fin lengths $L = 0.5$ and 0.75 while $\varepsilon_f < 1$ for $L = 0.25$ except for the lowest and highest fin positions. Fig. 11 (b) shows the fin effectiveness for $Ra = 10^4$. Fin effectiveness for $Ra = 10^5$ (not shown here) is similar to the case of $Ra = 10^4$. It can be seen that the fin effectiveness at any position H is lower than unity which indicates that using a fin under such conditions will reduce the heat transfer compared to the case with no fin. This is due to the effect of the low fin thermal conductivity ratio on the temperature distribution along the fin surface, which reduces the heat transfer from the fin surface. In addition, the fin suppresses the flow movement by blocking the flow below or above it. In general, the figures show that the fin effectiveness is generally found to attain minimum values when the fin is located at the center of the hot wall (i.e $H = 0.5$), for all values of fin length, except for the case of $Ra = 10^6$ where the fin effectiveness is approximately comparable away from the horizontal walls as seen in Fig. 11(c).

As the fin conductivity ratio increases, the fin effectiveness increases consequently which can be noticed in Fig. 12 for $R_k = 1000$. It is seen that for $Ra = 10^3$, the fin position has minor effect on the fin effectiveness for $L = 0.25$ and 0.5 which is similar to the case for $R_k = 10$, while for $L = 0.75$, the highest fin effectiveness is at $H = 0.5$. Fig. 12(b) shows that for $Ra = 10^4$, one can see that the fin position has significant effect on the fin effectiveness, indicating that the optimum position is near the lower or the upper surface while the poorest position is at $H = 0.5$. Fig. 12(c) shows that for $Ra = 10^5$, the fin has its optimum position near to the upper surface. Whereas for $Ra = 10^6$, the fin effectiveness changes slightly with the fin position and the optimum position is found at the center of the left wall (see Fig. 12(d)). One can see that at $R_k = 1000$, the fin length generally augments the fin effectiveness for all values of Ra. It is also noticed that using the long fin ($L = 0.75$) enhances heat transfer compared to the enclosure without a fin ($\varepsilon_f > 1$) for all values of Rayleigh number as seen in Fig. 12. The fin effectiveness at $R_k = 100$ which is not shown here, due to the paper size limitation, showed similar behavior as seen in Fig. 12 for $R_k = 1000$. However, the effectiveness values were smaller compared to the cases at $R_k = 1000$.

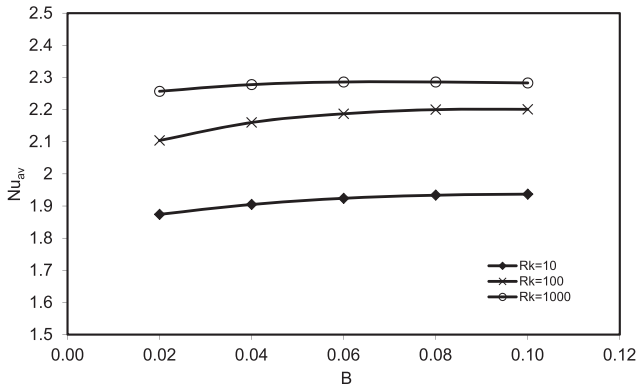

Fig. 9. The average Nusselt number as a function of fin thickness for ($H = 0.5$, $L = 0.5$ and $Ra = 10^5$).

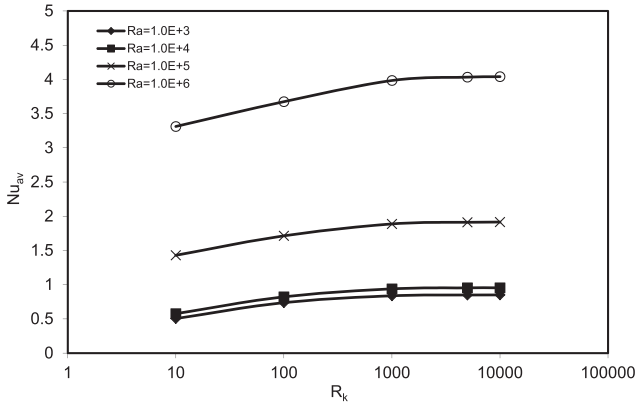

Fig. 10. The average Nusselt number as a function of conductivity ratio for ($H = 0.5$, $L = 0.75$, $B = 0.04$).

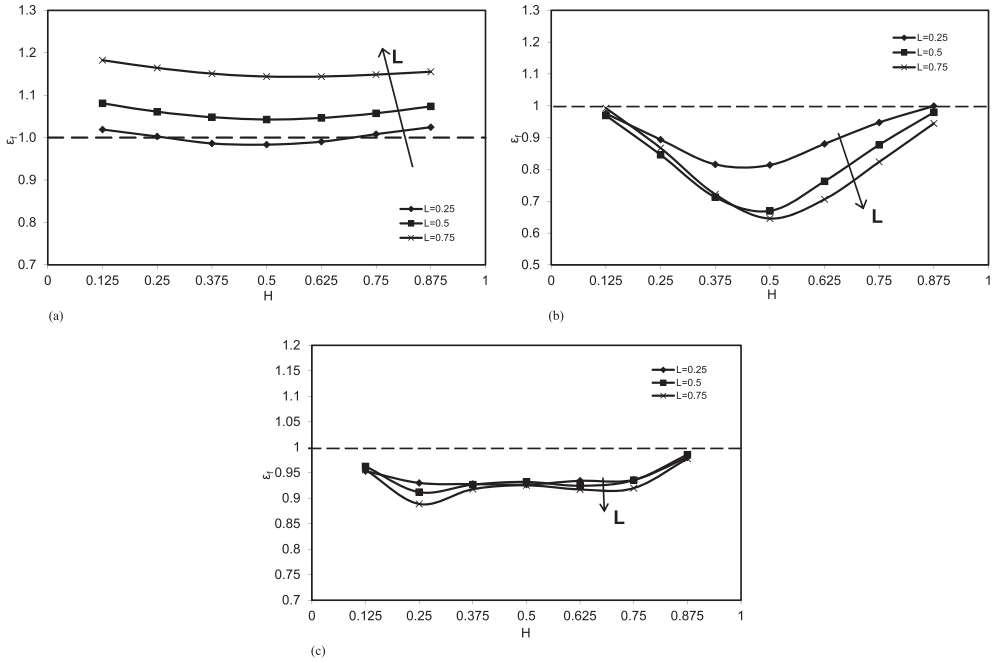

Fig. 11. Fin effectiveness as a function of fin position for $R_k = 10$ at (a) $Ra = 10^3$, (b) $Ra = 10^4$, (c) $Ra = 10^6$.

The fin length shows a noticeable effect on the fin effectiveness as seen in Figs. 11 and 12. For $R_k = 10$, the fin length enhances the fin effectiveness only for $Ra = 10^3$ as seen in Fig. 11(a), where conduction heat transfer is relatively dominant while heat transfer by convection is negligible. At these operating conditions, as the fin length increases, the conduction surface area increases which enhances heat transfer and consequently fin effectiveness as seen in Fig. 11(a). However, with the increase of Rayleigh number, convective heat transfer starts to become dominant over conduction, which makes the fin blockage a major factor in controlling heat transfer rate. At these conditions, the heat transfer suppression due to the fin blockage overcomes the augmentation due to higher Rayleigh numbers and this could be due to relatively lower fin temperature (i.e $R_k = 10$). Therefore, one can see that the fin effectiveness decreases with the increase of fin length as seen in Fig. 11(b and c). On the other hand, for $R_k = 1000$, the fin length increase enhances the fin effectiveness for all values of Rayleigh numbers as seen in Fig. 12. The enhancement in fin effectiveness with fin length for ($Ra = 10^3$, $R_k = 1000$) as seen in Fig. 12(a) is due to the same reasons as explained for the lower fin conductivity

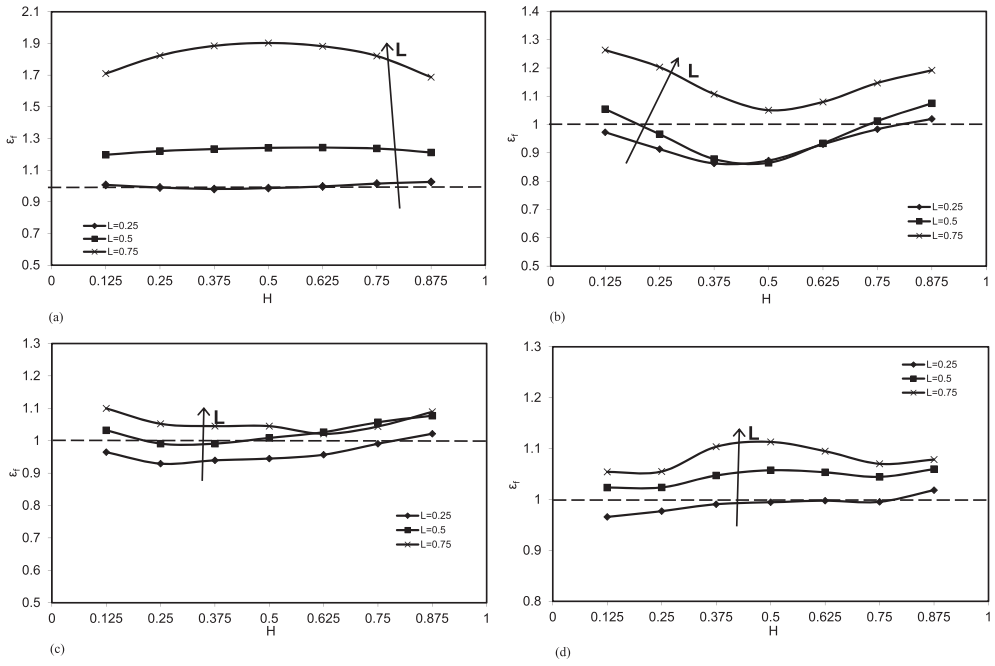

Fig. 12. Fin effectiveness as a function of fin position for $R_k = 1000$ at (a) $Ra = 10^3$, (b) $Ra = 10^4$, (c) $Ra = 10^5$, (d) $Ra = 10^6$.

ratio. While for higher Rayleigh numbers (Fig. 12(b)–(d)), a plausible explanation for the enhancement in fin effectiveness is that heat transfer enhancement at higher Rayleigh numbers overcomes heat transfer suppression due to the fin blockage effect and this is due to the fin higher surface temperature as seen in Fig. 6. This resulted in overall increase in heat transfer rate and consequently in fin effectiveness.

The location of minimum/maximum fin effectiveness along the left heated wall is strongly dependent on the relative weight of each factor that either suppresses or augments heat transfer. These factors as indicated earlier are: fin conductivity ratio, fin length, fin height along the left heated wall and Rayleigh number. There is a strong relation between both fin length and position and the blockage effect. One can see that at $Ra = 10^4$, the lowest fin effectiveness is located at the middle of left wall for all values of R_k and fin length. This shows that the fin blockage is maximum at $H = 0.5$ which in turn suppresses overall heat transfer. For higher values of Ra, there is no significant change of the fin effectiveness along the left wall. A plausible explanation is that the fin blockage effect has a relative negligible effect on heat transfer suppression compared to heat transfer enhancement at these higher Rayleigh number values. For the lowest Rayleigh number, it can be seen also that the fin effectiveness has no significant change along the left wall. This is due to the dominant conduction heat transfer which downplays fin blockage effect.

Figs. 11 and 12 indicate the noticeable effect of the fin length on the fin effectiveness. Therefore, it is beneficial to provide further analysis for the effect of fin length on the fin effectiveness. Fig. 13 presents the relation between the fin length and effectiveness at the lowest and highest Ra for $H = 0.5$. It can be noticed from Fig. 13(a) for $Ra = 10^3$ that the fin effectiveness is higher than unity for $L > 0.25$ for all conductivity ratio values. This is mainly due to the dominance of heat conduction over heat convection. For the highest Rayleigh number and lowest fin conductivity ratio, the fin effectiveness remains below unity for the whole range of fin length. Whereas for the higher conductivity ratios, the fin effectiveness is augmented with the increase of fin length and it becomes higher than unity at $L > 0.375$ and 0.25 for $R_k = 100$ and 1000 respectively. This is due to the significant effect of the fin conductivity ratio at high Rayleigh number. The figures also show that the fin effectiveness for lower Rayleigh numbers is significantly higher than that at high Rayleigh numbers especially with higher fin length. This is due to the blockage effect that the fin causes which hinders heat transfer where convection heat transfer is dominant.

The fin effectiveness is a reliable measure for how favorable it is to use a fin to enhance heat transfer inside a differentially heated cavity. The results show that when the heat transfer is dominated by conduction (i.e. low Rayleigh numbers), the fin effectiveness is higher than that of higher Rayleigh numbers. This is due to the fact that adding a fin will increase the heated surface area and consequently heat transfer. At low Rayleigh numbers, the fin blockage effect is negligible as shown earlier. Therefore, the fin effectiveness is enhanced. Moreover, this enhancement increases by increasing the fin length and conductivity ratio. However, at high values of Rayleigh number, heat is mainly transferred by convection. At these conditions, the fin blockage effect is playing a significant role in the flow circulation inside the cavity and as a result the fin effectiveness is lower.

Finally, a correlation for the average Nusselt number as functions of the effective system parameters (Ra and L) at different values of R_k is constructed in the following form.

$$\boldsymbol{Nu_{av} = a\, Ra^b L^c} \tag{16}$$

Where, the constants a, b and c are listed in Table 3. Fig. 14 presents a comparison between average Nusselt number from the numerical simulation and the one from the correlation for $H = 0.5$ and $L = 0.5$ at $Ra = 10^6$ for different values of R_k. The figure shows strong agreement between both results.

Table 3
Values of constants a, b, and c.

R_k	a	b	c	% Error	%Error STD
10	0.039	0.311	−0.4777	8.7	2.59
10^2	0.051	0.3021	−0.4154	7.8	2.19
$\geq 10^3$	0.055	0.3016	−0.363	7.6	2.96

6. Conclusion

Laminar natural convection inside square enclosures has been studied for enclosure with a horizontal fin attached to its hot wall at different positions. The present study focuses on the factors that affect heat transfer. The numerical results obtained can be summarized as follows:

1 The fin thickness has a minor effect on the heat transfer rate for $R_k = 10$ and 100 while it has almost no effect for $R_k = 1000$.
2 Increasing the conductivity ratio positively affects heat transfer from the finned hot surface for the range of $10 \leq R_k \leq 1000$, especially for a long fin, while the effect for $R_k > 1000$ is negligible.
3 The fin efficiency is suppressed by increasing the fin length and the rate of fin efficiency suppression increases with the decrease of R_k.
4 The fin effectiveness is enhanced by increasing R_k for all values of Rayleigh numbers. It is also found that in general, the fin effectiveness increases with the increase of the fin length.

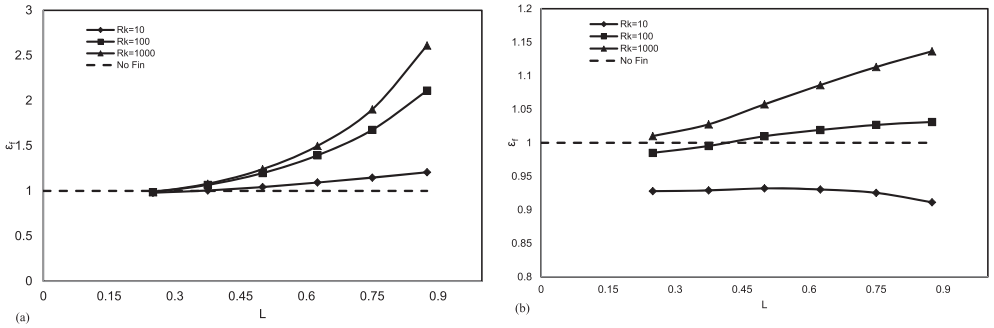

Fig. 13. Fin effectiveness as a function of fin length $R_k = 1000$ at (a) $Ra = 10^3$ and (b) $Ra = 10^6$.

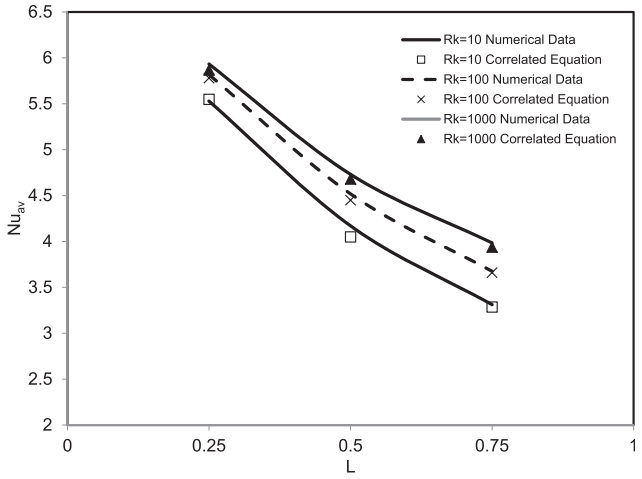

Fig. 14. Comparison between average Nusselt number form numerical results and correlation for $H = 0.5$ and $Ra = 10^6$.

5 The highest fin effectiveness values for a given fin length (L) and conductivity ratio (R_k) is found at the lowest Rayleigh number ($Ra = 10^3$) where conduction heat transfer is dominant inside the cavity and the fin blockage effect is negligible.

References

[1] D.A. Kaminski, C. Prakash, Conjugate natural convection in a square enclosure: effect of conduction in one of the vertical walls, Int. J. Heat Mass Transf. 29 (1986) 1979–1988.

[2] A. Liaqat, A.C. Baytas, Conjugate natural convection in a square enclosure containing volumetric sources, Int. J. Heat Mass Transf. 44 (2001) 3273–3280.

[3] Z.G. Du, E. Bilgen, Coupling of wall conduction with natural convection in a rectangular enclosure, Int. J. Heat Mass Transf. 35 (1992) 1969–1975.

[4] D.M. Kim, R. Viskanta, Heat transfer by conduction, convection and radiation across a rectangular cellular structure, Int. J. Heat Fluid Flow 5 (1984) 205–213.

[5] Abdullatif Ben-Nakhi, Mohamed A. Mahmoud, Conjugate natural convection in the roof cavity of heavy construction building during summer, Appl. Therm. Eng. 27 (2007) 287–298.

[6] B. Calcagni, F. Marsili, M. Paroncini, Natural convective heat transfer in square enclosures heated from below, Appl. Therm. Eng. 25 (2005) 2522–2531.

[7] Orhan Aydin, Ahmet Unal, Teoman Ayhan, Natural convection in rectangular enclosure heated from one side and cooled from the ceiling, Int. J. Heat Mass Transf. 42 (1999) 2345–2355.

[8] Mandar V. Joshi, U.N. Gaitonde, Sushanta K. Mitra, Analytical study of natural convection in a cavity with volumetric heat generation, ASME J. Heat Transf. 128 (2006) 176–182.

[9] S. Shakerin, M. Bohn, R.I. Loehrke, Natural convection in an enclosure with discrete roughness elements on a vertical heated wall, Int. J. Heat Mass Transf. 31 (1988) 1423–1430.

[10] Tzong-Huei Chen, Li-Yueh Chen, Study of buoyancy-induced flows subjected to partially heated sources on the left and bottom walls in a square enclosure, Int. J. Therm. Sci. 46 (2007) 1219–1231.

[11] Patrick H. Oosthuizen, Jane T. Paul, Natural convection in a rectangular enclosure with two heated sections on the lower surface, Int. J. Heat Fluid Flow 26 (2005) 587–596.

[12] C.J. Ho, J.Y. Chang, A study of natural convection heat transfer in a vertical rectangular enclosure with two-dimensional discrete heating: effect of aspect ratio, Int. J. Heat Mass Transf. 37 (1994) 917–925.

[13] Ramon L. Frederick, Natural convection in an inclined square enclosure with a partition attached to its cold wall, Int. J. Heat Mass Transf. 32 (1989) 87–94.

[14] E. Bilgen, Natural convection in cavities with a thin fin on the hot wall, Int. J. Heat Mass Transf. 48 (2005) 3493–3505.

[15] Xundan Shi, J.M. Khodadadi, Laminar natural convection heat transfer in a differentially heated square cavity due to a thin fin on the hot wall, ASME J. Heat Transf. 125 (2003) 624–634.

[16] Ramon L. Frederick, Alvaro Valencia, Heat transfer in a square cavity with a conducting partition on its hot wall, Int. Commun. Heat. Mass Transf. 16 (1989) 347–354.

[17] A. Nag, A. Sarkar, V.M.K. Sastri, Natural convection in a differentially heated square cavity with horizontal partition plate on the hot wall, Comput. Methods Appl. Mech. Eng. 110 (1993) 143–156.

[18] Syeda Humaira Tasnim, Michael R. Collins, Numerical analysis of heat transfer in a square cavity with a baffle on the hot wall, Int. Commun. Heat. Mass Transf. 31 (2004) 639–650.

[19] Abdullatif Ben-Nakhi, Ali J. Chamkha, Effect of length and inclination of a thin fin on natural convection in a square enclosure, Numer. Heat. Transf. Part A 50 (2006) 389–407.

[20] Abdullatif Ben-Nakhi, Ali J. Chamkha, Conjugate natural convection in a square enclosure with inclined thin fin of arbitrary length, Int. J. Therm. Sci. 46 (2007) 467–478.

[21] Xundan Shi, J.M. Khodadadi, Laminar fluid flow and heat transfer in a lid-driven cavity due to a thin fin, ASME J. Heat Transf. 124 (2002) 1056–1063.

[22] H. Oztop, E. Bilgen, Natural convection in differentially heated and partially divided square cavities with internal heat generation, Int. J. Heat Fluid Flow 27 (2006) 466–475.

[23] E. Bilgen, Natural convection in enclosures with partial partitions, Renew. Energy 26 (2002) 257–270.

[24] Ramon L. Frederick, Sergio G. Moraga, Three dimensional natural convection in finned cubical enclosures, Int. J. Heat Fluid Flow 28 (2007) 289–298.

[25] S.V. Patanker, Numerical Heat Transfer and Fluid Flow, Hemisphere Publishing Corp, New York, 1980.

[26] A. Nag, A. Sarkar, V.M.K. Sastri, Effect of thick horizontal partial partition attached to one of the active walls of a differentially heated square cavity, Numer. Heat. Transf. Part A (1994) 611–625.